URL: http://dx.doi.org/10.1016/j.ijfatigue.2009.01.010

Influence of woven ply degradation on fatigue crack growth in thin notched composites under tensile loading

M. Bizeul [a,*], C. Bouvet [b], J.J. Barrau [b], R. Cuenca [c]

[a] IGM – SUPAERO, 10 av E. Belin BP 54032 31055 Toulouse cedex 4, France
[b] IGM – Université Paul Sabatier, 118 route de Narbonne 31062 Toulouse cedex 4, France
[c] Eurocopter France, 13725 Marignane, France

Keywords:
Woven fabric composite
Fatigue
Crack propagation
Linear elastic fracture mechanics

A B S T R A C T

This paper deals with the fatigue of the through-the-thickness crack propagation in thin notched composite laminates made of two glass woven plies. It highlights the different crack growths between warp and weft directions of the woven ply. Experimental results show a decrease of the crack growth rate per cycle with the increase of the crack initiation time. Moreover, it has been shown that it is necessary to take into account the fatigue damage of the woven plies in term of loss of rigidity in the initiation phase. The fatigue crack growth rates are then quantified using Paris law type equations and linear elastic fracture mechanics (LEFM).

1. Introduction

Woven fabric composites are being used as primary structural parts in several aeronautical applications. Due to weight reduction, the skin of such structures is often thin and a through-the-thickness crack can appear over the period of service. This macro-crack may be due to defects during manufacturing process, impact or stress concentration. To assess the damage tolerance of such structures with a through-the-thickness crack under fatigue loading, it is thus necessary to characterize the fatigue crack propagation.

These structures are subjected to complex loading conditions but the tension–tension cyclic loading seems to be the worst in term of crack propagation. Some authors investigated the fatigue crack propagation in glass fibre reinforced polymer. Pegoretti et al. [1] studied fatigue crack growth behaviour of polypropylene composites reinforced with short glass fibres and examined how the crack growth varied with fibre content and frequency of the sinusoidal applied load. Experiments were conducted on a single-edge notched tension specimen at room temperature. It was observed that the crack growth rate decreased as the crack length increased in the early stage of the fatigue test. A Paris type law was identified in using strain energy release rate amplitude. Shindo et al. [2] examined the room temperature and low temperatures fatigue behaviour of notched plain woven glass laminates under mode I loading. For all specimens, the weft fibre bundles were aligned with the load axis. Load control fatigue tests were performed with Compact Tension specimens and additionally SEM observations of the crack were performed. Crack lengths were calculated from the compliance data obtained during test using finite element analysis. Three stages of fatigue crack growth were identified: crack initiation, stable crack growth and unstable crack propagation. Optical micrograph of fatigue crack path taken at approximately $N/N_f = 90\%$ showed an amount of damage near the crack tip especially at low temperatures. The damage zone consisted of matrix cracks in the undulation region. Therefore, as the size scale of damage that occurred was not small compared to the other significant dimensions, J-integral was used and the crack growth rate was related to ΔJ through a power law relationship.

However, few works were conducted on relatively thin laminates. The objective of this work is to describe the fatigue propagation of a through-the-thickness crack in notched laminates made of two woven glass plies aligned with the load direction. The influence of the tows nature (warp or weft) of the woven ply on the crack growth is studied and the crack initiation duration influence on the propagation law coefficients is evaluated.

2. Material and experimental details

The material used in this research is glass/epoxy woven composite. The studied laminates are made of two 8-harness satin balanced woven fabric (8-HS) pre-pegs plies with a fibre volume fraction of 50%. The two plies are aligned with the load direction and two kinds of laminates are studied whereas warp or weft tows are in tension. The stacking sequence is $[0/90]_2$. To initiate a through-the-thickness crack, the test specimen is notched with a 0.2 mm diameter diamond thread. The fatigue tests are conducted in strain control at room temperature (about 20 °C) at a frequency

* Corresponding author.
E-mail addresses: bizeul@supaero.fr (M. Bizeul), barrau@cict.fr (J.J. Barrau).

of 20 Hz. The imposed strain levels are $\varepsilon_{min} = 10^{-3}$ and $\varepsilon_{max} = 3 \times 10^{-3}$. This maximum fatigue strain level corresponds to the infinite life asymptote in *S–N* curve [3–7] and is widely used as design fatigue strain for structures made of glass plies. The specimen is cooled down to room temperature by a fan and its temperature is monitored (the thermocouple sensor is located 10 mm under the notch). No increase in temperature was recorded.

The skins of aeronautical structures are often constrained to spar strain. To represent the real loading conditions, a test specimen with an unidirectional carbon fibres strip on one edge has been developed. Moreover, it reduces the likelihood that global inelastic strains occur under fatigue loading. The characteristics of the test specimen are summarized in Fig. 1. The stacking sequence of woven laminate is $[0/90]_2$.

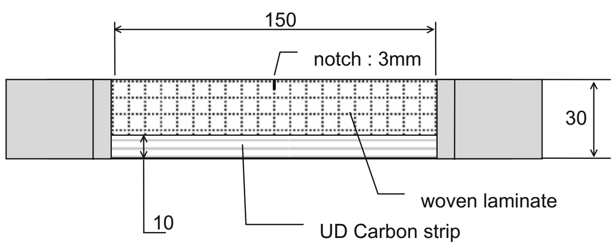

Fig. 1. Fatigue test specimen characteristics.

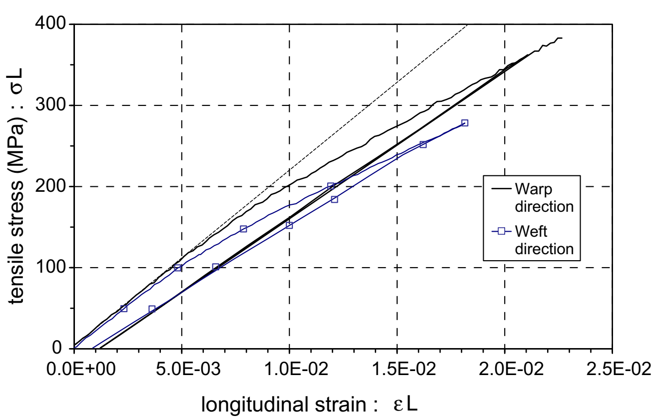

Fig. 2. Stress–strain curves of warp and weft direction $[0/90]_2$ glass woven laminates.

Fatigue tests are performed on a INSTRON 10 kN closed-loop servo-hydraulic tension machine with an extensometer with a 50 mm gage length on the carbon strip to control strain level. The crack growth is monitored with the help of a CCD camera. Due to the relative transparency of the glass fibres reinforced plastics, the propagation of a white damage zone by back-illumination is observed. This kind of phenomenon was also described by [5,8].

The microscopic examinations reveal the presence of fibre tows breakage and through-the-thickness crack all along the damage zone (Fig. 3). In front of the damage zone, the microstructure is safe. As [4,6,9] stated, it is observed that tows breakage occur preferentially in the crimp zones.

First, the static mechanical properties of the woven glass material are given in Table 1. The woven ply is balanced and the tensile elastic modulus for both warp and weft directions are approximately equal. The ultimate tensile strength is influenced by the tow type: weft direction is more undulated and knee-point in this direction is earlier than warp one (Fig. 2). The warp tow is considered to run straighter than weft one.

The tensile behaviour curves of both warp and weft directions are shown in Fig. 2. The warp direction being straighter than the weft one results in a greater ultimate tensile stress. Finally, inelastic strains appear with high stress conditions as the unloading paths previous to failure show.

3. Results and discussion

Fatigue crack propagation in thin woven laminates of stacking sequence $[0/90]_2$ is influenced by the tow type. The crack growth is first analysed in laminates with warp tows in tension and next in weft laminates. The crack length corresponds to the white damage zone length; the microscopic study shows that tows breakage and through-the-thickness crack exist all along the damage zone.

3.1. Fatigue crack growth in the warp direction

Fig. 5 presents crack growth versus cycles for warp laminates. Due to specimens width and notch length, the maximum crack length is around 17 mm. In accordance with previous results [1,2,10], crack propagation starts from the "initiation" phase (sometimes called "stage I"): crack length does not exceed 2 mm and the crack growth rate is slow. Then it continues with the "propagation" phase of stage II (where the Paris law is supposed to hold) where the rate is important up to the last stage where the carbon strip influence leads to crack arrest. The main fact underlined by these results is the large dispersion between sam-

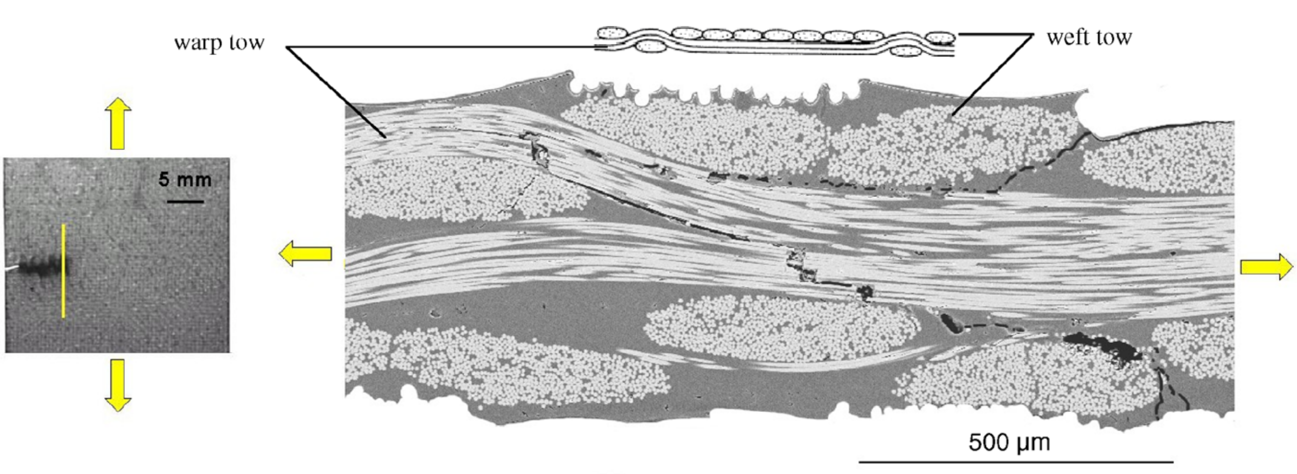

Fig. 3. Through-the-thickness crack and tow breakage in the tip of the visible damage zone.

Table 1
Static mechanical properties of the studied woven ply.

Tow type	Warp	Weft
Elastic modulus E (MPa)	21500 ± 100	21000 ± 300
Tensile strength σ_{UTS} (MPa)	385 ± 15	280 ± 5

ples. The number of cycles to failure is five times greater for the slowest sample than the fastest one. The related crack growth rates exhibit same curve shape: it points out the typical decrease of crack growth rates when the crack length is about 2 mm. This typical behaviour is common in metal alloys [10] and associated with long crack initiation and was also observed in short-glass fibre reinforced polypropylene [1]. In previous work [11], this slowing down is compared to tows width and associated with the influence of microstructure on the beginning of crack growth. Owing to digital image correlation, the study of the beginning of crack growth is carried out (Fig. 4). The important jump in displacement field allows to identify crack tip. As the tow width measures 0.5 mm (Fig. 3), the crack growth becomes steady when around three or four tows are cut. The dispersion in crack growth results could also be explained by the position of the notch tip compared to the unit cell of the woven plies. Unfortunately, due to stacking sequence and manufacturing process and small tow width, it was not possible to put the notch tip in the same position with respect to microstructure for each specimen test. Despite the large dispersion in experimental results, it is possible to establish a relationship between the initiation duration and the crack growth rates level.

3.2. Fatigue crack growth in the weft direction

The crack growth in weft laminates is similar to previous ones and presents the three stages stated before (Fig. 6). Nevertheless, the initiation stage lasts three times greater than warp ones. The number of cycles to failure is nearly ten times greater for the slowest sample than the fastest one. In the same way, the crack growth

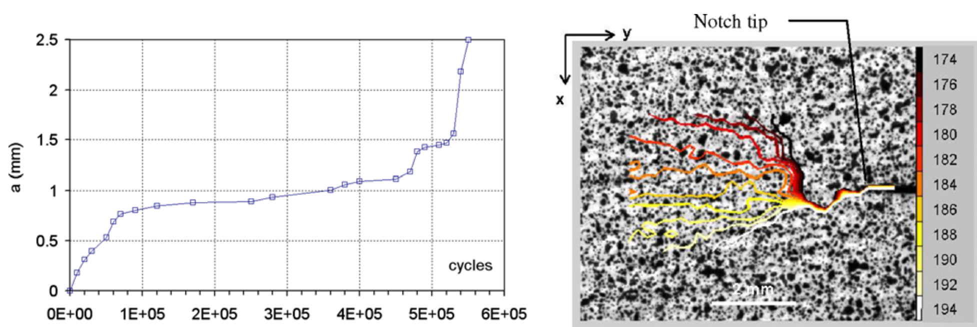

Fig. 4. Early crack length variation obtained by digital image correlation.

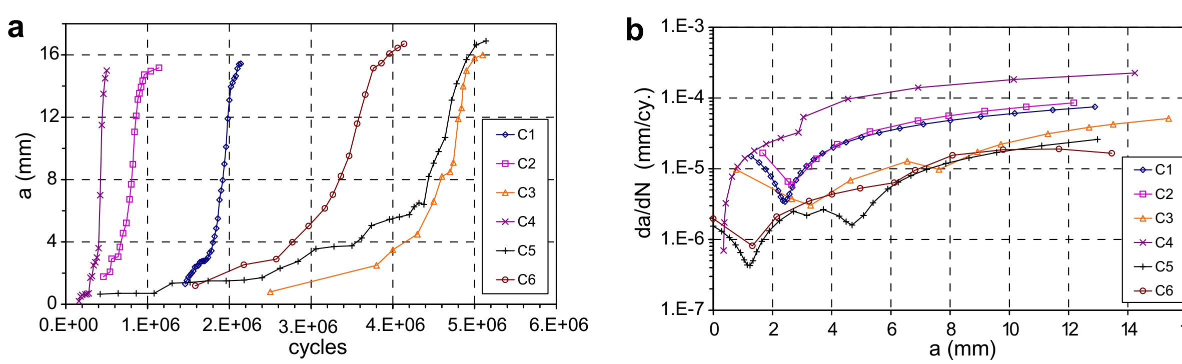

Fig. 5. Length variation: (a) crack growth rate and (b) in fatigue for $[0/90]_2$ warp laminates.

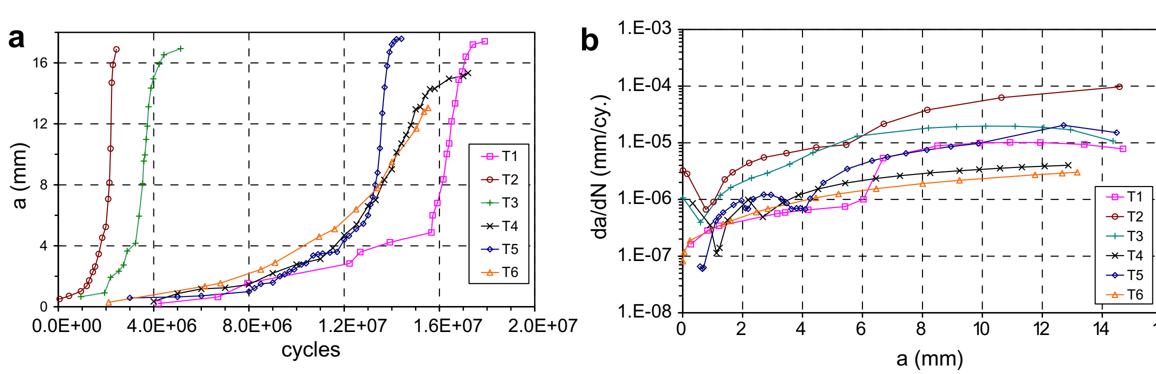

Fig. 6. Length variation: (a) crack growth rate and (b) in fatigue for $[0/90]_2$ weft laminates.

dispersion is important and initiation duration varies by a factor of ten between the six samples. By looking at the crack growth rate, it can be said that the microstructure influence seems to stop when the crack length is about 2 mm like warp results. It can also be emphasized that greater the length of fatigue test greater is the delay in stage II beginning.

4. Crack growth law identification

In a first attempt, the crack growth is modelled with the help of the linear elastic fracture mechanics through the use of the strain energy release rate G. This does not take into account the pronounced material heterogeneity. However, any extensive matrix damage was observed in front of the crack tip. In addition, since the crack always grows along the perpendicular direction to the load, the assumption that the crack runs in mode I has been made (Fig. 3).

Since the initiation duration is not easy to control and seems to act upon crack growth rates, the experimental results with crack lengths between 2 mm and 14 mm are only retained. The influence of the carbon strip on crack growth rate begins at this last crack length limit. Thus, the identified law hereafter does not describe the initiation stage and the decrease due to carbon strip.

In the other hand, it is known that the longitudinal modulus of woven glass plies changes with the increase in cycles [4,6,12,13]. The fatigue process of the composite is usually found to have three stages: (1) rapid modulus decay with cycles (2) gradual modulus decay and (3) another rapid modulus decay in the last few cycles for higher loading conditions. The rapid modulus decay at the beginning of the fatigue process is caused by the initiation and accumulation of debonds in the weft and matrix cracks. This behaviour is similar to that commonly observed in orthotropic laminates; however, the woven system behaviour differs in that debonds occur at each region surrounding a fibre undulation. Therefore, the damage is not localized in the laminate [14]. The damage evolution in fatigue of unnotched woven laminates of $[0/90]_2$ stacking sequence without carbon strip in warp and weft directions is investigated. The fatigue tests parameters are kept constants in connection with fatigue propagation tests: the fatigue tests are led in strain control at two different maximum strain levels with a ratio $R_\varepsilon = \varepsilon_{min}/\varepsilon_{max} = 0.33$ (Fig. 7). At least three specimens are tested for each fatigue strain level. The stages identified before are distinguished. Fatigue tests performed at $\varepsilon_{max} = 3 \times 10^{-3}$ do not present the last stage that lead to failure. The maximal fatigue strain level $\varepsilon_{max} = 6 \times 10^{-3}$ is chosen according to the typical knee-point in static tensile tests and is equal to the corresponding static strain for the weft direction (the corresponding strain to knee-point in warp direction is about $\varepsilon = 8 \times 10^{-3}$). No inelastic strains are observed at these two fatigue strain levels. In both cases, it is obvious that the longitudinal modulus of woven glass material decreases. The softening is more important in the weft direction most probably due to the greater undulation of this tow. As the maximum fatigue strain increases, the modulus decay grows. These results enable to understand that the initiation duration is greater in the weft direction than in the warp direction: the softening in the vicinity of the notch limits the fibre stress and delays the through-the-thickness crack initiation.

It is possible to describe the previous experimental curves (Fig. 7) of the fatigue modulus decay of unnotched woven plies without carbon strip at maximum strain $\varepsilon_{max} = 3 \times 10^{-3}$ with the following laws (E_0: static tensile modulus at 0 cycle, E_N: tensile modulus after n cycles and N: number of cycles):

– in warp direction:

$$\frac{E_N}{E_0} = 1.20N^{-0.017} \quad \text{for } N \in [10^4; \infty[\tag{1}$$

– in weft direction:

$$\frac{E_N}{E_0} = 1.34N^{-0.031} \quad \text{for} N \in [10^4; \infty[\tag{2}$$

The initiation duration of a through-the-thickness crack in the notched specimens with carbon strip is not easy to control and is not the same for each specimen. As shown by the graph in Fig. 7, this period of time acts upon the stiffness of the woven plies and hence on the sample stiffness. To evaluate the correct value of energy release rate G in each sample, it is necessary to take in to account the fatigue modulus decay of thewoven plies. As the initiation duration corresponds to at least 70% of the fatigue crack growth tests duration and that woven modulus decay reaches an asymptotic value quickly, the assumption is made that the degradation of the woven plies modulus just takes place during the initiation duration of a through-the-thickness crack. The typical decrease of crack growth rate associated with the end of microstructure influence identifies the initiation duration and by extent the woven damaged modulus E_N with Eqs. (1) or (2) for each specimen. Owing to a linear finite element model with composite shell elements, the energy release rate G is determined for several values of crack lengths (Fig. 8). With the help of fracture mechanics and experimental results, the assumption is made that the crack grows in mode I. A mesh similar to FE model of Coats [16] is used in the vicinity of crack tip. The mesh refinement is chosen according to

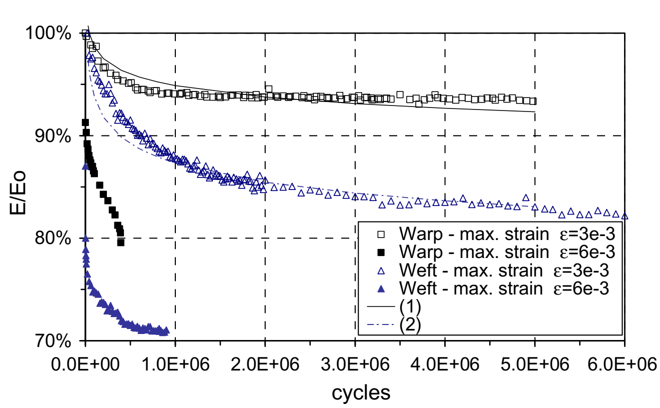

Fig. 7. Modulus decay in fatigue of the warp/weft direction of the studied glass woven ply.

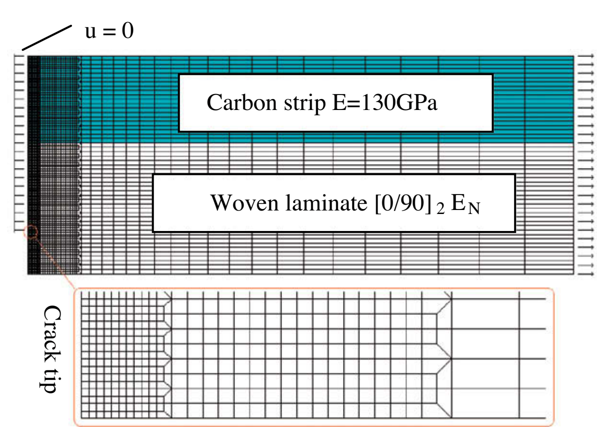

Fig. 8. 2D finite element model.

the convergence of energy release rate value. From the first loading of the notched strip specimen the initial modulus E_0 of the woven ply is calculated. The modulus value E_N of woven plies is deduced from Eqs. (1) and (2) and the number of cycles of initiation N. The energy release rate variation $\Delta G_I = G_I^{max} - G_I^{min}$ is obtained from Virtual Crack Extension method [15]. However, the modelling of modulus decay for strains greater than $\varepsilon = 3 \times 10^{-3}$ does not affect energy release rate significantly because of the localization in the crack tip. Therefore, only the modulus decay at fatigue strain level of woven plies in the notched strip specimen is modelled.

Finally, the fatigue crack growth rates are quantified according to the Paris Law in terms of the crack growth exponent (m) and coefficient (C). All results presented hereafter are for crack growth rate da/dN in mm/cycle and strain energy release rate G_I in kJ/m^2.

$$\frac{da}{dN} = C \cdot (\Delta G_I)^m \qquad (3)$$

Fig. 9 shows that Paris law equation corresponds well with experimental results for warp laminates by looking at correlation coefficients values. The (m) exponent value of Paris law is around 2. On the other hand, coefficient (C) decreases as the crack initiation duration increases and varies between $C = 10^{-6}$ and $C = 1.3 \times 10^{-7}$.

For weft laminates, the fatigue crack propagation law (Fig. 10) shows good agreement with experiments. The (m) exponent value of Paris law is also around 2 whereas coefficient (C) varies between $C = 1.2 \times 10^{-7}$ and $C = 8.5 \times 10^{-8}$. It can be seen that the Paris law coefficients of the slowest warp laminate are equal to the fastest weft laminate. As for warp laminates, the fastest specimen in weft direction has the highest value of coefficient (C).

Furthermore, to investigate the range of these identified propagation laws, some fatigue tests on notched specimens without car-

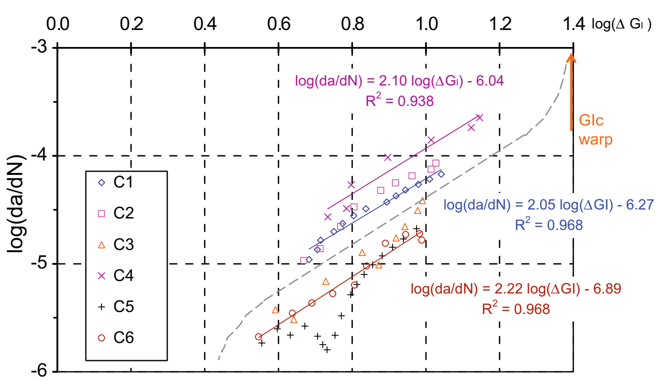

Fig. 9. Paris law identification for $[0/90]_2$ warp glass woven laminates.

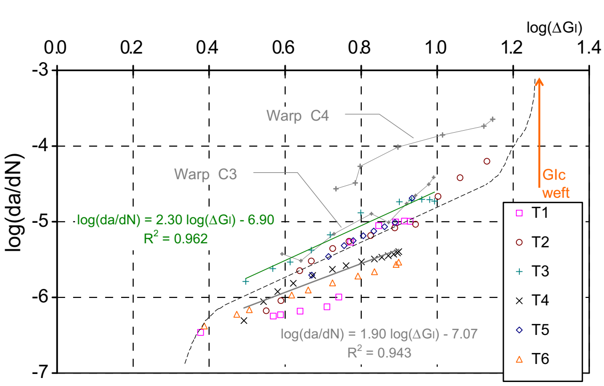

Fig. 10. Paris law identification for $[0/90]_2$ weft glass woven laminate.

Table 2
Critical energy release rates G_{Ic} in warp and weft $[0/90]_2$ laminates.

Tow type	Warp	Weft
G_{Ic} (kJ/m^2)	26.2 ± 3	20.2 ± 2

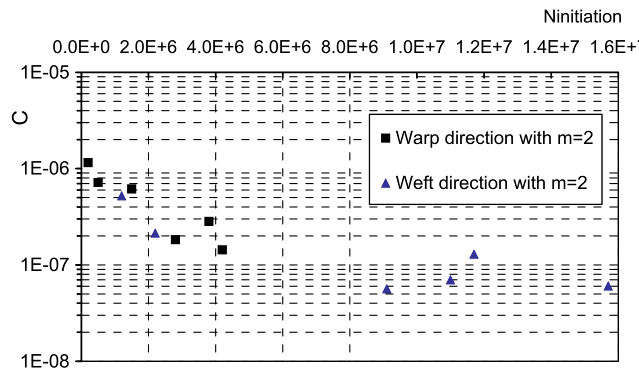

Fig. 11. Values of C Paris law coefficient for warp and weft specimens.

bon strip are carried out to estimate the critical strain energy release rates in both warp and weft laminates made of two woven plies. Three samples for each direction are tested in a similar manner than strip specimens and only the maximum fatigue strain level is changed ($\varepsilon_{max} = 4 \times 10^{-3}$) to reduce test duration. The crack growth is monitored continuously with CCD camera and the fatigue test is stopped when the crack is about 3 mm length.

In order to evaluate G_{Ic}, these fatigue samples are tested in static at a rate of V = 1 mm/min. and the ultimate tensile load is recorded. Owing to the previous described FE model, it is possible to assess the value of G_{Ic} (Table 2).

Table 2 highlights that the critical strain energy release rate in warp direction is greater than in weft direction; it is in agreement with the fact that warp tows are straighter than weft tows. These results underline that the fatigue crack propagation previously detailed hold in stage II.

The exponent m of the Paris law seems to be independent of the type of fibres of the studied woven ply. On the other hand, the coefficient (C) varies in a large range whether in the warp or weft direction. The results show that a relationship may exist between this coefficient and the crack initiation duration. In proceeding to linear regressions with a coefficient (m) taken as constant and equal to $m = 2$, the different coefficients (C) of the Paris law of each specimen are calculated. Fig. 11 plots the values of coefficient (C) in function of the crack initiation duration that corresponds to the typical decrease of crack growth rate. It can be seen that the coefficient (C) of the Paris law is independent of the type of fibres (warp or weft) of the studied woven ply and depends only on the initiation duration.

As the warp direction presents less modulus decay and as the warp tows are straighter, the initiation duration in this direction is limited. When the crack initiation duration in weft direction is similar to that of warp direction, the coefficient (C) of the Paris law of weft laminates is closed to the one of warp laminates. Nevertheless, it is noted that weft laminates are longer to initiate.

5. Conclusions

Fatigue crack propagation in woven laminates made of two plies has been investigated. The following conclusions can be reached:

– The through-the-thickness crack initiation duration is difficult to control. This results in important experimental dispersions.
– The crack growth rate exhibits a typical decrease associated with microstructure influence. This phenomenon disappears when the crack length exceeds 2 mm.
– Paris type law with strain energy release rate is appropriate to model fatigue crack propagation. Nevertheless, it is necessary to take into account the damage of the woven plies by fatigue modulus decay. For $[0/90]_2$ orthotropic laminates the exponent m of the propagation law is nearly equal to 2. In addition, the coefficient (C) varies with the crack initiation duration. On average, weft direction of the studied woven plies is longer to initiate.
– The use of strain energy release rate hides the phenomenons in the crack tip. It does not allow to separate the fatigue matrix damage of the residual strength of glass fibres. Further developments are expected.

Acknowledgements

The authors would like to thank Eurocopter France and EADS CRC for their financial and technical support during this research.

References

[1] Pegoretti A, Ricco T. Fatigue crack propagation in polypropylene reinforced with short glass fibres. Compos Sci Technol 1999;59:1055–62.
[2] Shindo Y, Inamoto A, Narita F. Characterization of mode I fatigue crack growth in GFRP woven laminates at low temperatures. Acta Mater 2005;53:1389–96.
[3] Shindo Y, Takano S, Horiguchi K, Sato T. Cryogenic fatigue behavior of plain weave glass/epoxy composite laminates under tension–tension cycling. Cryogenics 2006;46:794–8.
[4] Pandita S, Huysmans G, Wevers M, Verpoest I. Tensile fatigue behaviour of glass plain-weave fabric composites in on – and off-axis directions. Compos: Part A 2001;32:1533–9.
[5] Xiao J, Bathias C. Damage and fracture of notched non-woven and woven composites laminates. Compos Sci Technol 1994;52:99–108.
[6] Fujii T, Amijima S. Microscopic fatigue processes in a plain-weave glass-fibre composite. Compos Sci Technol 1993;49:327–33.
[7] Talreja R. Fatigue of composite materials: damage mechanisms and fatigue-life diagrams. In: Fatigue of composite materials, Technomic, Lancaster, PA; 1987.
[8] Belmonte H, Manger C, Ogin S, Smith P, Lewin R. Characterisation and modelling of the notched tensile fracture of woven quasi-isotropic GFRP laminates. Compos Sci Technol 2001;61:585–97.
[9] Osada T, Nakai A, Hamada H. Initial fracture behavior of satin woven fabric composites. Compos Struct 2003;61:333–9.
[10] Pugno N, Ciavarella M, Cornetti P, Carpinteri A. A generalized Paris' law for fatigue crack growth. J Mech Phys Solids 2006;54:1333–49.
[11] Bizeul M, Bouvet C, Barrau JJ, Cuenca R. Warp and weft degradation influence of glass woven ply on fatigue crack growth in notched composites. In: Proceedings of JNC15, Marseille 6–8; June 2007. p. 409–16.
[12] Schulte K, Reese E, Chou TW. Fatigue behaviour and damage development in woven fabric and hybrid fabric composites. In: Matthews FL, Buskell NCR, Hodgkinson JM, Morton, J. editors. In: Proceedings of the Sixth International Conference on Composite Materials (ICCM-VI) and Second European Conference on Composite Materials (ECCM-II), 20–24 July 1987, vol. 4. London, UK: Elsevier; 1987, pp. 489–99.
[13] Naik R, Patel S, Case S. Fatigue damage mechanism characterization and modelling of a woven graphite/epoxy composite. J thermoplast compos mater 2001;14.
[14] Alif N, Carlsson LA. Failure mechanisms of woven carbon and glass composites. Composites materials: fatigue and fracture. 6th vol; 1997. p. 471-93 [ASTM STP 1285].
[15] Rybicki EF, Kanninen MF. A finite element in linear fracture mechanics. Int J Num Met Eng 1978;10:25–35.
[16] Coats T, Harris C. A progressive damage methodology for residual strength predictions of notched composite panels. Nasa/TM-1998-207646.